Mikrochim. Acta 138, 133–152 (2002)

Mikrochimica Acta
© Springer-Verlag 2002
Printed in Austria

X-Ray Microanalysis of Thin Surface Films and Coatings

Jean-Louis Pouchou

ONERA – Department of Metallic Materials and Processes, 29 avenue Division Leclerc – BP 72–92322 Châtillon, France

Abstract. The paper gives an overview of the present knowledge in the field of X-ray analysis of surface films and more generally stratified specimens. The aim of the paper is not to report the details and formulas of the available quantitative procedures, but to concentrate on the general ideas and orders of magnitude illustrating the capability and limits of the method, and on the optimal adaptation of the operating conditions to every particular problem. The various specific pitfalls which can be encountered are pointed out, in particular the fluorescence effects when using high-energy X-ray lines, or the anomalies due to chemical bonding, absorption uncertainties, and contamination effects when soft radiations are employed.

Key words: X-ray microanalysis; in-depth analysis; surface layer; layered specimen.

Since the early times of X-ray microanalysis, there was a temptation for characterising surface segregations (e.g. [1]), but it has been necessary to wait until the mid-80's to see a few groups produce a sufficient effort for developing reliable general models and dedicated software, in order to properly characterise layered micro volumes by X-ray microanalysis [2, 3]. In fact, the real starting point for the current use of this technique is the early '90s, when more modern, friendly and powerful software tools were developed and became commercially available [4, 5]. Before that period, only a few experts deeply involved in surface films and stratified specimens were using X-ray microanalysis for this purpose [6]. But since that time, a significant number of laboratories in the world have been using X-ray microanalysis to determine composition and/or mass thickness of near-surface layers, in the range ~ 0.1 to 1 $\mu g/cm^2$. In this context, not only electron probe micro analysers (EPMA) but also analytical scanning electron microscopes (EDS/SEM) are now used to produce meaningful results.

After ten years of experience, the comparisons made by several authors have shown clearly that the method favourably competes with the technique of ion backscattering (RBS), commonly considered as the reference method for measuring near-surface segregations in the sub-micron thickness range. In most cases, comparisons of X-ray microanalysis with RBS have shown that both techniques agree within less than 10%. In some cases, X-ray microanalysis may be superior because it may avoid some limitations of RBS due to overlapping effects. The weakness of both techniques occurs for buried layers consisting of very light elements: in the case of RBS, such layers do not have a strong efficiency for scattering the incident particles; in the case of X-ray analysis, the soft characteristic lines that are emitted are strongly absorbed by the upper layer(s) and may be undetectable if the layers are buried too deeply below the surface.

The aim of the present paper is to give an overview of the capability of X-ray microanalysis applied to layered specimens, without entering into the details of the models and formulas which can be found in the literature, both for the author's models [7] and for others [8, 9]. The specific aspects of X-ray analysis applied to layered specimens will be emphasised, by comparison with the conventional analysis of homogeneous specimens, and the main sources of errors and limitations of the method will be pointed out.

Analysed Depth: Choosing the Electron Energy and the Analytical Line

– Roughly, the full range of electrons is given by $R_0 \approx \alpha E_0^{1.78}$, where E_0 is the electron energy in keV, and R_0 is in mg/cm^2. For all elements, the proportionality factor α is of the order of 10^{-2} (actually, it increases slightly with the atomic number Z). Hence, at 1 keV, which is the lowest electron energy that can practically be used for analytical purpose, the full range is of the order of 0.01 mg/cm^2 (i.e. $\sim$10 nm for a material which would have a density equal to 10). It would be $\sim$0.6 mg/cm^2 at 10 keV, $\sim$2 mg/cm^2 at 20 keV, and $\sim$7 mg/cm^2 at 40 keV. The full range R enabling the excitation of a particular atomic level with energy E_c, is equal to $R \sim \alpha\ (E_0^{1.78} - E_c^{1.78})$.
– The penetration (or projected range) is not very different from the full range (or path) in very light targets (because they weakly scatter the incident electron beam), but it is typically half of the path in the heaviest targets (because of the strong electron scattering). When the atomic number of the material increases, the increase of the electron scattering compensates more or less the fact that the full range (expressed in units of mass per unit surface) is longer. Thus, at a given accelerating voltage, the depth of penetration of the incident electrons is almost the same whatever the nature of the target, when it is expressed in mg/cm^2 or $\mu g/cm^2$. This property is in fact the main reason why the problems of layered specimen analysis can be solved by means of automatic iterative procedures, as will be mentioned later: whatever the complex structure of a layered specimen and the distribution of the elements as a function of depth (which is the unknown), a good approximation of the depth of primary excitation can be obtained at any voltage, so that the computation procedure can be initialised properly.
– From the expression of the range, it is obvious that the depth of excitation can be strongly reduced by using an electron accelerating voltage E_0 close to the critical energy E_c of the atomic level of interest. For most elements (except light elements with Z less than 20), two series of characteristic lines are available in practice for the analysis: the K and L lines for the medium-Z elements, the L and M lines for the heaviest ones. The excitation thresholds for both series widely differ, typically by an order of magnitude. In conventional analysis applied to homogeneous specimens, high-energy lines are most often used, because they are not strongly absorbed inside the specimen and are easier to measure. On the contrary, in the case of layered specimens, the choice of a high- or low-energy analytical line should depend on the nature of the problem. If a deeply buried layer has to be analysed, high-energy electrons have to be used, in order to generate the emission of high-energy photons, able to be detected after passing through the over-layer(s) without strong absorption. On the contrary, if the problem consists in analysing thin segregations close to the surface, the best efficiency will be obtained with a low-energy line analysed at low accelerating voltage. In this case, the resolution in depth is much better than if high-energy lines were used at low over-voltage ratio, because of the higher slowing-down of the electrons at low energy. Let us take the case of a medium-Z element such as zinc to illustrate that obtaining a low depth of analysis is much easier by using the Lα line ($E_c = 1.021$ keV) at low voltage than the Kα line ($E_c = 9.66$ keV) at a higher voltage. Lets us imagine first that the Zn Lα line is excited by 2 keV electrons. In such conditions, the depth of excitation does not exceed $\sim$15 $\mu g/cm^2$ (i.e. $\sim$20 nm). On the other hand, in the energy region just above the Zn K threshold, the electron slowing-down is about five times lower. Hence, to get the same analysed depth with the Kα line, one should operate at a very low over-voltage ratio, corresponding to an electron energy of 9.82 keV. Because the ionisation cross-sections are maximum when the over-voltage ratio is between $\sim$2 and 3 and rapidly decrease to zero when the over-voltage tends to unity, the number of generated Kα photons would finally be $\sim$30 times less than the Lα ones, in spite of the lower fluorescence yield of L levels. Moreover, the excessively low over-voltage ratio for the Kα radiation would lead to a peak-to-background ratio unacceptably bad (a few units for the pure element, even by WDS spectrometry). Table 1 illustrates the better resolution in depth obtained when combining soft X-rays and low-energy electrons, by comparing the influence of an increase of 100 eV (a reasonable step in practice) of the energy of the incident electrons in the vicinity of 2 keV (for the Zn Lα line), and in the vicinity of 10 keV (for the Zn Kα line). It can be seen that in the

Table 1. Comparison of the operating conditions required to produce the same maximum excitation depth (15 μg/cm^2) for two characteristic lines of different series (Zn Lα and Zn Kα in pure zinc). Computations made with the XPP model [7]

Electron energy (keV)	Line	Over-voltage ratio	Full electron range		Maximum ionisation depth		Mean ionisation depth	
			(μg/cm^2)	(nm)	(μg/cm^2)	(nm)	(μg/cm^2)	(nm)
2	Zn Lα	1.959	23	32	*15*	21	4.3	6.0
2.1	Zn Lα	2.056	26	36	17	24	4.7	6.6
9.82	Zn Kα	1.017	51	714	*15*	21	5.2	7.3
9.92	Zn Kα	1.027	52	729	25	35	7.4	10.4

low-energy situation, a step of 100 eV for the electron energy only increases the ionisation depth for Zn L by 3 nm, whereas at high energy the corresponding increase is five times greater for the K level.

Sensitivity to Surface Segregations

Although X-ray microanalysis cannot be considered as a technique for surface analysis, because the minimum depth from which measurable X-rays can be produced is never less than ~10 to 20 μg/cm^2 (i.e. ~50 to 100 nm in the lightest solid targets and ~5 to 10 nm in the heaviest ones), it enables to detect small surface segregations because of its good signal-to-background ratio, especially when wavelength dispersive spectrometers (WDS) are used rather than energy dispersive spectrometers (EDS). It has already been shown experimentally [4] in the case of copper on silicon substrate, that segregations less than 0.1 μg/cm^2 (i.e. ~0.1 nm pure Cu) can be detected by WDS using the low-energy Cu Lα line. Even by EDS, segregations less than 0.2 μg/cm^2 can be detected in the same conditions. For very light elements, the surface sensitivity is also interesting: for example, the surface oxidation of a freshly polished aluminium block can be easily measured: using 3 keV incident electrons and a multi-layer monochromator for the O Kα line, the peak-to-background ratio for a ~6 nm oxide film (i.e. ~1 μg/cm^2 oxygen) approximately equals 4, which means that again, oxygen surface segregations as low as 0.1 μg/cm^2 can be detected by WDS. With EDS, the sensitivity to very light elements is slightly worse, but may still reach some tenths of a μg/cm^2.

Obviously, the drawback of this surface sensitivity is that measurements, mainly at low-voltage, are strongly influenced by all kinds of uncontrolled surface imperfections of the specimens and standards: dirt, oxidation, contamination under the beam, etc. Let us imagine the case where a freshly produced layer of a Zn compound (supposed to be perfectly clean) would be analysed using as a reference an "old" standard having a layer of ZnO oxide on it. Table 2 shows the relative error on the Zn Lα analysis that would result from the oxidation of the standard, as a function of both voltage and oxide thickness (in the range 5 to 20 nm).

Sensitivity to Buried Segregations

There is some difficulty to define in a few words the capability of detecting buried segregations, because each case is a particular case. So, let us first recall some basic facts:

- A buried segregation can be detected only if at least one of its constituent elements can be excited with sufficient efficiency by the incident electrons. This implies that a minimum energy of the electron beam has to be employed. This also means that the maximum depth where primary X-ray excitation may occur is limited by the maximum accelerating voltage available in most EPMA or SEM columns, i.e. ~40 kV. At this maximum voltage, the ultimate electron penetration is of the order of 4 mg/cm^2 whatever the nature of the target. This means that

Table 2. Relative errors on the Zn Lα relative intensity, which can result from the use of an imperfect Zn standard covered with an oxide film. Computation performed with the XPP model [7]

ZnO thickness (nm)	2 keV	3 keV	5 keV	10 keV	15 keV	20 keV	30 keV	40 keV
5	7.7%	3.3%	1.35%	0.6%	0.45%	0.4%	0.36%	0.35%
10	16.2%	7.1%	2.8%	1.2%	0.9%	0.8%	0.73%	0.7%
20	30%	15.2%	6.1%	2.5%	1.8%	1.6%	1.5%	1.4%

usable information can be collected from regions located at a depth not exceeding $\sim 2\,\mathrm{mg/cm^2}$, provided that the radiation can emerge.

– Supposing that the buried material has been excited, a characteristic radiation of at least one of the elements of this material should emerge with sufficient intensity out of the specimen. Here, the limiting phenomenon is the absorption of X-rays in the specimen itself. Because mass absorption coefficients for the usable lines may differ by 3 to 4 orders of magnitude, depending on the nature of emitting and absorbing elements, the situation differs noticeably from one case to another. However, it is evident that high-energy radiations (weakly absorbed) should preferably be used to get information coming from deeply buried regions. Unfortunately, light and very light elements emit only soft radiations, which are significantly absorbed in almost all kinds of target.

In the examples below, it will be assumed that reasonable analytical conditions are realised (i.e. conditions able to provide meaningful results) when it is possible to measure a k-ratio (relative to pure bulk standard) of at least 10% for a pure buried material.

Case of a Substrate

The case of a substrate (semi-infinite buried material) will be illustrated first. Figure 1 represents the maximum mass thickness of the over-layer that can cover a pure substrate and still let it emit a relative intensity (or k-ratio) of 10% at any voltage in the operating range of the instrument (i.e. typically 1 to 40 kV). Since this result does not depend too strongly on the scattering properties of the surface material, the computation has been done for a medium-Z layer ($Z = 30$). The maximum acceptable mass thickness of this upper layer is evaluated for the characteristic lines of 4 different substrates, covering the 0–10 keV X-ray energy range: C K (0.284 keV), Al Kα (1.559 keV), Ti Kα (4.966 keV) and Au Lα (9.713 keV). Especially for the low-energy radiations, the result is sensitive to the absorption of the radiation in the upper layer. Hence, for each radiation, the computation has been done at 40° take-off with different hypothetic values of the mass absorption coefficient μ/ρ, which cover the typical m.a.c. range of every radiation in all possible absorber elements.

Figure 1 shows that for most radiations, except for the soft radiations for which $\mu/\rho > 1000\,\mathrm{cm^2/g}$, the maximum over-layer thickness which enables a pure substrate to have a k-ratio of 10% lies between ~ 0.5 and $\sim 2\,\mathrm{mg/cm^2}$. For substrates emitting softer radiations, the over-layer should most often be less than $\sim 0.5\,\mathrm{mg/cm^2}$ in order to guarantee a sufficient k-ratio coming from the substrate.

Case of a Buried Layer of Finite Thickness

In the same manner as for a substrate, we can look at the maximum over-layer thickness of a medium-Z element that can cover a pure buried layer of particular thickness and let this buried layer emit a k-ratio of 10% at any voltage between 1 and 40 kV. The computation has been done for 4 values of the buried layer thickness: 1000, 100, 10 and $2\,\mu\mathrm{g/cm^2}$. For simplicity, one can define the burying factor as the ratio of the over-layer mass thickness to that of the buried pure layer for which a k-ratio of 10% can be obtained (at 40° take-off in the present calculation).

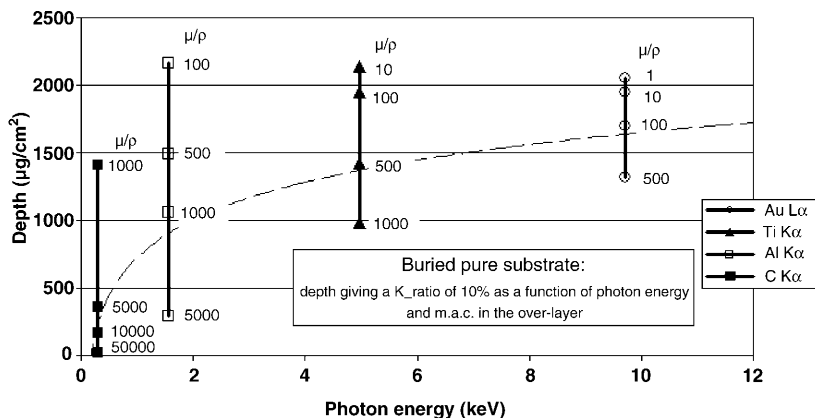

Fig. 1. Maximum thickness of an over-layer (with Z ~ 30) enabling a pure substrate to reach a 10% k-ratio (relative to pure standard) between 1 and 40 kV, as a function of the energy of the radiation and of its absorption coefficient in the over-layer (40° take-off assumed)

– Figure 2 shows that for a very thick layer (1000 μg/cm^2) the burying factor is between ∼1 to 2 in all cases where the absorption coefficient of the measured radiation by the over-layer is not too high, i.e. $\mu/\rho < 5000\,\mathrm{cm^2/g}$. To excite efficiently such a thick buried layer, a high value of the voltage would be necessary: in this particular situation, the value of 10% for the k-ratio would be obtained at the highest voltage available, i.e. 40 kV. Otherwise, when soft radiations are involved with higher absorption coefficients, the burying factor is less than 1, i.e. the maximum depth for the analysis of a thick buried layer should not exceed a fraction of the mass thickness of the layer itself. In this situation, the 10% k-ratio would be reached at some lower voltage, typically between ∼20 and 40 kV.
– When the buried layer has an intermediate thickness (100 μg/cm^2), Fig. 3 shows that, whatever the energy of the radiation measured, the burying factor is most often between ∼2 and 4, which means that the buried layer can be reasonably measured when it is covered by ∼2 to 4 times its own mass thickness. In this situation, the k-ratio would reach a maximum of 10% between ∼15 and 40 kV. For the softer radiations with $\mu/\rho > 5000\,\mathrm{cm^2/g}$, the burying factor is ∼1 or less, which means that the maximum depth acceptable is of the order of the thickness of the buried layer, or sometimes less for extreme absorption. In this situation, the k-ratio would reach a maximum at low voltage, typically between ∼8 and 15 kV.
– For a thinner buried layer (10 μg/cm^2), the situation is not very different, except that the influence of the absorption is less pronounced for soft radiations. Figure 4 shows that most often (except for the highest absorption), the burying factor lies between ∼2 to 5. Even when the absorption is high ($\mu/\rho \sim 10000\,\mathrm{cm^2/g}$), a buried layer of 10 μg/cm^2 can still be analysed when it is covered with a similar thickness of material. In the situations of

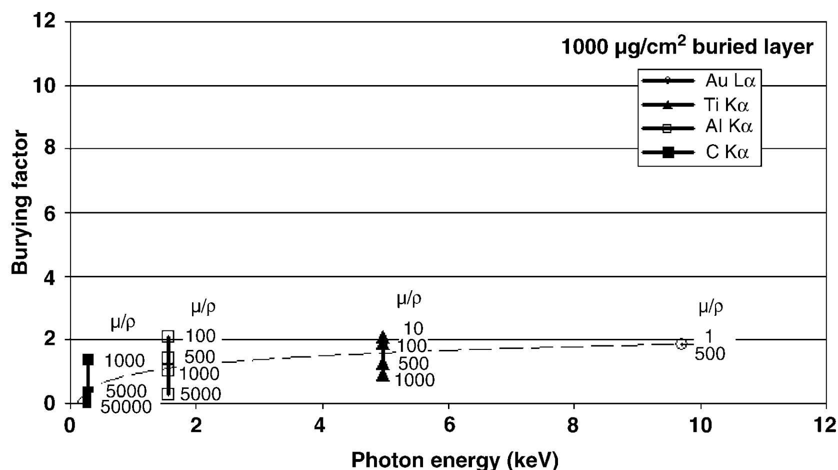

Fig. 2. Burying factor for a 1000 μg/cm^2 buried layer, as a function of the energy of the radiation and of its absorption coefficient in the over-layer (40° take-off assumed). The burying factor is defined as the maximum mass thickness of an over-layer (relative to that of the buried layer) which enables a buried layer of pure material to reach a 10% k-ratio (relative to pure standard) between 1 and 40 kV

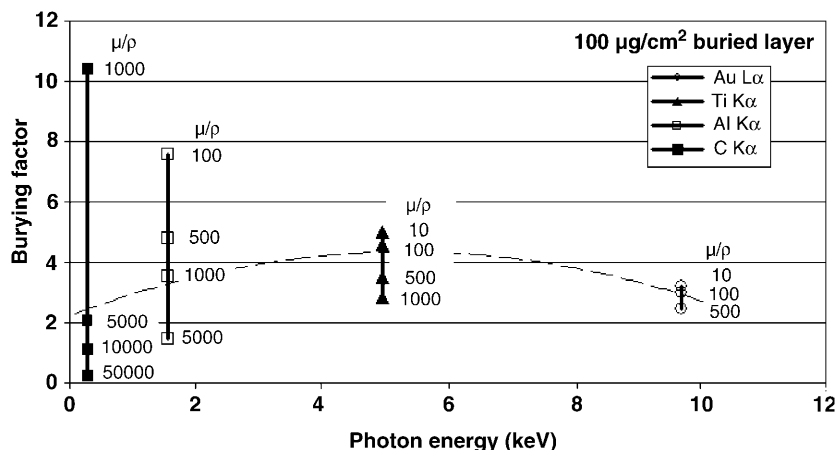

Fig. 3. Burying factor for a 100 μg/cm^2 buried layer, as a function of the energy of the radiation and of its absorption coefficient in the over-layer (40° take-off assumed). The burying factor is defined as the maximum mass thickness of an over-layer (relative to that of the buried layer) which enables a buried layer of pure material to reach a 10% k-ratio (relative to pure standard) between 1 and 40 kV

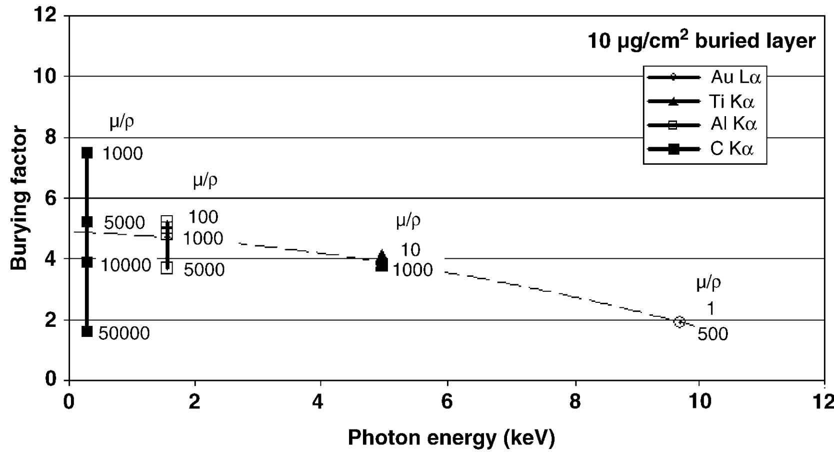

Fig. 4. Burying factor for a $10\,\mu g/cm^2$ buried layer, as a function of the energy of the radiation and of its absorption coefficient in the over-layer (40° take-off assumed). The burying factor is defined as the maximum mass thickness of an over-layer (relative to that of the buried layer) which enables a buried layer of pure material to reach a 10% k-ratio (relative to pure standard) between 1 and 40 kV

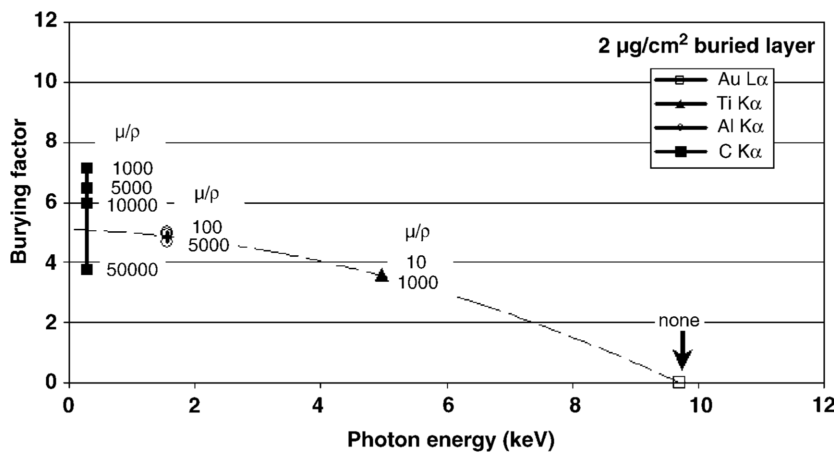

Fig. 5. Burying factor for a $2\,\mu g/cm^2$ buried layer, as a function of the energy of the radiation and of its absorption coefficient in the over-layer (40° take-off assumed). The burying factor is defined as the maximum mass thickness of an over-layer (relative to that of the buried layer) which enables a buried layer of pure material to reach a 10% k-ratio between 1 and 40 kV

Fig. 4, the k-ratio reaches a maximum of 10% at a voltage between ~3 and 12 kV.

– Finally, for a very thin buried layer ($2\,\mu g/cm^2$), one comes to a situation more favourable for low-energy radiations than for high-energy ones: as shown on Fig. 5, it is not possible to reach a 10% k-ratio for a gold buried layer by using the Au Lα line (9.713 keV critical energy), because this would require an over-voltage ratio much too low, i.e. not usable in practice. On the contrary, even when the absorption coefficients are high ($\mu/\rho \sim 10000\,cm^2/g$), the softer radiations of the buried layer can be detected at a depth equal to ~4 to 6 times the mass thickness of the buried layer itself.

The general conclusion of this chapter is that the maximum depth at which a layer can be buried while being measurable is closely dependent on the mass thickness of the buried layer itself. It depends also on the absorption of the emitted radiation in the upper material. Most often, the maximum depth at which a buried layer can be reasonably measured is ~2 or 3 times the mass thickness of the layer itself (see Table 3).

Table 3. Burying factor as a function of mass thickness of the buried layer and of the radiation emitted by this layer. Burying factor characterises the capability of analysing a buried layer. It is defined as the ratio of the maximum over-layer thickness to that of the buried layer which still enables to measure "comfortably" the buried layer. The criterion for "comfortable" measurement is that a pure buried layer should yield a k-ratio of 10% (relative to pure element standard) at any voltage in the available range of the instrument (typically 1 to 40 kV)

Radiation energy	Thickness of buried layer			
	$2\,\mu g/cm^2$	$10\,\mu g/cm^2$	$100\,\mu g/cm^2$	$1000\,\mu g/cm^2$
< 2 keV	4–7	1–7	0.1–10	0.1–2
2–8 keV	3–5	3–4	2–5	0.5–2
8–10 keV	0–3	2–3	2–3	1.5–2

Higher burying factors would be obtained in the rare cases of thin buried layers measured with soft X-rays moderately absorbed by the upper material. Lower values would be obtained either for thick layers emitting strongly absorbed soft X-rays, or on the opposite, for very thin layers measured with high-energy lines.

Specific Problem with High-Energy Lines: Secondary Emission by Fluorescence

In all situations of X-ray microanalysis using high-energy lines, significant secondary emission due to fluorescence (excited by the continuum and possibly by characteristic lines) takes place. In conventional quantitative software for analysing homogeneous volumes, the fluorescence excited by lines is usually taken into account by a simplified model (e.g. [10]), whereas the fluorescence by the continuum is most often neglected, because it is assumed (perhaps wrongly) that it has almost the same relative contribution in the specimen as in the standard, so that it should approximately cancel when forming the k-ratio. However, there is one case of homogeneous specimen analysis where the fluorescence by the continuum has definitely to be incorporated into the computation: it is the case of the standardless analysis (standardless meaning here that purely theoretically computed standards are used), since the relative contribution of the fluorescence by the continuum to the intensity of a standard may reach several tens of percent for the lines with highest energy that can be used [11].

In the case of stratified specimens, omitting the fluorescence effects would lead to unacceptable errors, because they would be not only quantitative, but also qualitative. Very simple and common cases of analysis can lead to strong errors if fluorescence effects are omitted. A typical case is the analysis with high-energy lines of thick surface layers (i.e. layers thicker than the ultimate depth of excitation by the electrons), erroneously assumed to be thick enough to be analysed in a classical way, i.e. like an homogeneous volume. A typical example of this kind is the analysis of $\sim 5\,\mu m$ Zn-Ni coatings on Fe substrate, or any similar case where the element(s) of the layer have atomic number(s) slightly higher than the element(s) of the substrate. Accurate measurements of the fluorescence effects have been reported in the case of a Cu layer on Ni substrate [12].

In the present paper, the influence of the secondary emission by fluorescence is illustrated by Fig. 6, in the simple case of a $2\,\mu m$ pure Ge film on pure Cu substrate. To show the specific contribution of each phenomenon, the predicted k-ratio curves versus accelerating voltage are computed for the Kα lines of the layer and the substrate in three conditions: (i) without taking into account the fluorescence (i.e. primary excitation by the electrons only), (ii) by adding the effect of the fluorescence excited by the characteristic lines, and (iii) by adding the fluorescence excited by the continuum. The considerable influence of the

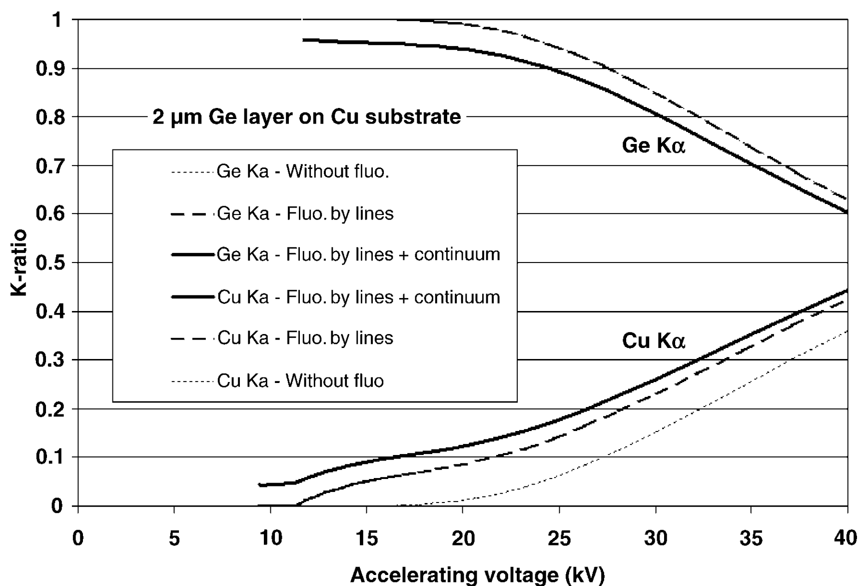

Fig. 6. Influence of the fluorescence excited by characteristic lines and by the continuum on the k-ratios of a specimen made of a thick Ge layer ($2\,\mu m$) on Cu substrate. Computation made for the Kα lines using XPP model

fluorescence on the measured k-ratios can be appreciated in Fig. 6: even when the measurements are made at 15 kV (where the primary excitation volume is completely included in the surface film), one gets a Cu Kα relative intensity of almost 10% coming from the substrate, one half due to the excitation by characteristic Ge K lines of the layer and the other half due to the excitation by the continuum (below the Ge K level, for example at 10 kV, only the continuum is able to produce secondary emission of the Cu substrate, which leads to k-ratio close to 5% for Cu Kα). Reciprocally, if one considers the X-ray emission of the Ge layer below $\sim$17 kV (which is the voltage at which electrons begin to cross the interface with a residual energy greater than the Ge K level), one can observe that the k-ratio for the Ge Kα line is not equal to unity, but typically 5% lower. This lack of emitted intensity represents the fraction of the total Ge Kα emitted radiation which would come, in a semi-infinite Ge target, from the secondary radiation excited by the continuum in the regions deeper than 2 μm in the present example. Normally, in this situation, a scrupulous analyst should be aware of the heterogeneity of the specimen, since a conventional correction procedure applied to this layered specimen would lead to a sum of concentrations close to 104%.

What would happen in the opposite geometry, i.e. in the case where the heavier element (Ge) is the substrate, and the lighter (Cu) is in a 2 μm layer on top? Figure 7 shows that the contribution of the fluorescence of Cu by Ge K lines is weaker than in the previous geometry, and that the fluorescence by the continuum contributes by $\sim$2% to 2.5% to the emission of the Ge substrate and to the lack of Cu emission, which is apparent between $\sim$12 kV and $\sim$23 kV (it can be noted that this voltage range, where the primary excitation volume is entirely included in the film, is wider than in the previous example, because the mass thickness corresponding to a linear thickness of 2 μm is significantly higher for Cu than for Ge). This geometry, in which the excitation by the continuum is the main source of secondary X-ray emission, is very dangerous, because the lack of emission of the layer is almost exactly compensated by the emission of the substrate. Hence, if such a specimen was analysed at 20 kV with conventional procedures, on the pretext that it looks homogeneous for incident electrons below $\sim$23 kV, an erroneous composition would result: for example $\sim$97.3 wt% Cu and 2.8 wt% Ge at 20 kV. The danger of this result is that the sum of the resulting concentrations is very close to 100%, so that there is no indication for an error in the procedure, as opposed to the previous example (Ge on Cu substrate). Moreover, as mentioned before, the danger of such a situation is that it could lead not only to a wrong quantitative result, but also to a serious qualitative mistake, since it could lead to the conclusion that the material is an alloy, while it is a stratified specimen! In the present example, the only way to detect the heterogeneity of the specimen would be to make a second measurement at a higher voltage, for example 40 kV, where the k-ratio of the layer significantly decreases, while that of the substrate increases because of the emergence of the primary emission.

But if one imagines a thicker Cu layer, for example 4 μm, on top of a Ge substrate, it would be impossible, even at 40 kV, to generate enough primary excitation

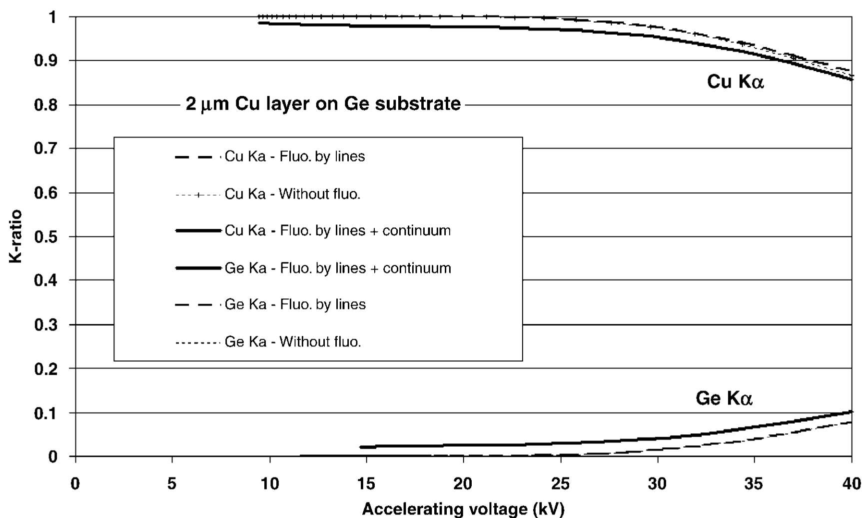

Fig. 7. Influence of the fluorescence excited by characteristic lines and by the continuum on the k-ratios of a specimen made of a thick Cu layer (2 μm) on Ge substrate. Computation made for the Kα lines using XPP model

in the substrate to observe a change in the k-ratios. Hence, there would be no evidence that the measured k-ratios ($\sim$99% to $\sim$98% for Cu Kα and $\sim$0.6% to 1.5% for Ge Kα in the range 12–40 kV) could result from a stratified specimen rather than an homogeneous compound.

To conclude this chapter, it can be said that it is a wise attitude, every time a fluorescence effect is suspected, to confirm the high-energy lines measurements, every time it is possible, with extra measurements made with the low-energy lines, which are much less sensitive to the fluorescence effects.

Specific Problems with Low-Energy Lines

Low-energy X-rays are of a real interest for the analysis of layered specimens, since they are more sensitive to the near-surface regions, and almost not influenced by the fluorescence effects. However, great care should be taken when using these lines, for different reasons:

- A peculiar problem occurs with the L lines of the 3d transition metals (Sc to Ni), or the M lines of the 4f transition elements, because their specific characteristics of emission and absorption may change drastically as a function of the chemical bonding, i.e. with the composition of the material to be analysed. For example, if one considers the case of nickel (probably the most critical situation in the 3d transition series), the specific number of Ni Lα photons generated per electron interacting with a Ni atom is greater for a Ni atom bonded with an element such as Al than for a Ni atom in the pure material. At the same time, the partial filling of the Ni 3d band by Al 3p electrons produces a decrease of the self-absorption of the Ni Lα line by Ni atoms (the anomaly of Ni Lα self-absorption tends to vanish when Ni is bonded with Al). The combination of both effects tends to produce (above some voltage) a stronger Ni Lα intensity emerging from a nickel compound than from the pure material! Hence, for these transition elements, the low-energy lines can be used without any danger only in the cases where the layers involved are made of pure material or when bulk standards with the same composition as the layers are available (in the latter situation, the effective mass absorption coefficients for these bulk compounds should have been evaluated first, for example through measurements of the emerging intensity versus accelerating voltage).
- A second problem is due to the change of the peak shape that can occur either (i) as a function of the accelerating voltage, or (ii) as a function of the chemical bonding.
  - (i) In the case of the Lα lines of transition elements for example, the absorption edge is located in the short-wavelength side of the line. Hence, when the absorption increases by increasing the accelerating voltage, the measured line distorts in a progressive manner, so that its maximum seems to shift towards long-wavelengths.
  - (ii) In the case of ultra-light elements, for example carbon, chemical bonding has a strong influence on the peak position and intensity distribution of the emission band. In WDS measurements, this has to be taken into account. Let us imagine for example a pure carbon layer on top of a silicon carbide substrate: the pure carbon will exhibit a wide C K emission band, whereas the strong Si–C bonding will produce a much narrower C K peak in the carbide (the area-to-peak shape factors can differ by several tens of percent, the precise value depending on the spectral resolution of the monochromator used). Hence, at any voltage sufficient for the carbon atoms of the substrate to be excited, the measured carbon signal will be a mixture of both characteristic lines, so that the shape of the resulting line will become continuously narrower when increasing the voltage. Hence, a measurement of the area-to-peak factor at every voltage will be necessary to approximately compensate for this effect. Obviously, when the spectrometer is scanned for a long time to perform the area-to-peak measurements, care should be taken to avoid surface contamination by carbon, which could (again) be a strong source of errors.
- The surface contamination (mainly by carbon, but also by oxygen and silicon) under the beam may be a source of difficulty when soft X-rays are used for the analysis. In the electron microprobes, the anti-contamination devices (a combination of air jet + liquid N_2 cold trap) are generally efficient, and capable of eliminating most of the contamination. However, in the case where carbon surface films have to be measured, it should first be verified that the combined action of incident electron beam and

air jet does not produce the destruction of the layer itself ! From our experience, it seems that such a deterioration can occur more easily for thin carbon deposits (∼10 to 20 nm) made by ion-sputtering techniques than for films with similar thickness obtained by thermal flashing.

In scanning electron microscopes, the situation is different: the contamination is most often a very strong limitation to serious quantitative measurements of very light elements, especially carbon and also nitrogen (because of the very strong absorption of N Kα by carbon). The following example of EDS carbon measurements on Fe_3C, in a microscope equipped with a turbo-molecular pumping system, illustrates the importance of the problem. After acquiring a spectrum during 1000 seconds (the time needed to obtain a well defined spectrum) on a fixed point of the specimen, we obtained a carbon k-ratio of ∼ 9.3%, i.e. ∼ 5 times higher than expected for Fe_3C in these operating conditions (15 kV and 35° take-off). By performing an automated acquisition sequence with stage control, reducing the acquisition time per point T and increasing by the same factor the number N of acquisition locations (in order to keep constant the product N.T), and after summing the N spectra acquired, we obtained 2.5 times the expected k-ratio with 5 acquisitions of 200 seconds, almost twice the expected result with 10 acquisitions of 100 seconds, and finally a satisfactory result by summing 100 acquisitions of 10 seconds each [12]. If the carbon contamination was uniformly distributed under the beam (which in fact is not true), the above results would represent an amount of contamination of ∼ 4 μg/cm^2 (i.e. ∼ 20 nm) after 100 seconds, more than ∼ 6 μg/cm^2 (i.e. ∼ 30 nm) after 200 seconds, and ∼17 μg/cm^2 (i.e. ∼ 85 nm) after 1000 seconds!

– Finally, a recurrent problem with the soft X rays is the precise knowledge of their absorption coefficients, in particular every time the analytical line has an energy close to an absorption edge of a major element of the specimen. For low-energy photons, the mass absorption coefficients have values ranging typically from thousands to tens of thousands cm^2/g. For a typical m.a.c. of ∼10000 cm^2/g, one should be aware that changing the m.a.c. by 1% produces a change of ∼1% in the emerging intensity. It can be considered that presently, every modern quantitative package provides for the most common emission lines and absorbing elements a set of sufficiently reliable m.a.c.s to enable (in association with a given model) to perform quantitative analysis with an accuracy of the order of 5% or less. However, in particular cases (i.e. mainly when the energy of the characteristic line is very close to an absorption edge of an heavier element), the m.a.c. values of the tables may be completely wrong. In such cases, the analysis of layered specimens can be a good method to get a reliable value for a given m.a.c.. Some examples have already been mentioned [13]. One of the most didactic is probably the determination of the absorption of Hg Mα (2.196 keV), Hg Mβ (2.283 keV), S Kα (2.307 keV) and S Kβ (2.464 keV) lines by gold atoms, because all these lines, which have similar energies, are in the vicinity of the Au M_{IV} and M_V absorption edges (respectively 2.220 and 2.307 keV). The technique consists in depositing a gold layer with an adequate thickness (typically 200 to 300 μg/cm^2) over one part of an HgS crystal (cinnabar), and to analyse this layered specimen at variable voltage. Using the Au Mα k-ratios and a dedicated thin film program, the mass thickness of deposited gold can be determined with a reasonable accuracy (probably ∼ 5%). Then, the theoretical k-ratio curves for the substrate elements can be computed using the default set of m.a.c.s (in our case the m.a.c.s of Heinrich's tables [14]) and compared to the experimental k-ratios formed by using the uncoated area of the HgS crystal as a reference (actually, the HgS crystal was coated with a thin carbon film prior to gold deposition, in order to avoid charging effects on the part of the specimen without gold). The result for all theses lines having almost the same energy (which means that they should have almost the same behaviour if their absorption coefficients were the same) is the following:

– For the weakly absorbed Hg Mα line (the energy of which is lower than the Au M_V edge), and for the strongly absorbed S Kβ line (the energy of which is higher than the Au M_{IV} edge), there is a good agreement between the computed and the experimental k-ratios. Hence, the μ/ρ values proposed for these lines by Heinrich's tables (respectively 984 and 2852 cm^2/g) are confirmed experimentally.
– On the contrary, for Hg Mβ and S Kα lines which are close to the Au M_{IV} edge, one observes

a strong discrepancy between the computed and the measured variation of the k-ratios versus voltage: the computed k-ratios are much too low for S Kα, and much too high for Hg Mβ, compared to the measured ones (which are very close for both lines). This experiment, where several lines of similar energy behave differently because of their absorption coefficients, demonstrates unambiguously the capability for X-ray microanalysis to extract more accurate m.a.c. values than some of the tabulated ones. From this experiment, the following values were deduced: $\mu/\rho_{\text{(S K}\alpha\text{ in Au)}}$ $\approx 2200\,\text{cm}^2/\text{g}$ (instead of $3380\,\text{cm}^2/\text{g}$ from Heinrich's table), and $\mu/\rho_{\text{(Hg M}\beta\text{ in Au)}}$ $\approx 2170\,\text{cm}^2/\text{g}$ (instead of $1427\,\text{cm}^2/\text{g}$ from Heinrich's table).

Quantitative Procedures for Analysing Stratified Specimens

– All quantitative procedures for characterising composition and/or layer thickness in stratified specimens involve (ab initio or a posteriori) the distribution in depth of the primary ionisations produced by incident electrons (the function usually called $\phi(\rho z)$ since the pioneering work of Castaing [15]). The principal property of this function is that its integral is proportional to the number of generated ionisations on the atomic level of interest, the most important proportionality factor being the value of the ionisation cross-section $Q_j(E_o)$ at the initial energy E_o. In the case of layered specimens, the partial integration of $\phi(\rho z)$ from one layer limit to the other gives the X-ray intensity generated in this particular layer. The main effort to define the $\phi(\rho z)$ function with a reasonable accuracy in a wide range of operating conditions and for all kinds of materials has been done during the 80's, and most modern software programs based on this concept have been developed in the 90's. Three main types of approaches can be distinguished:

(i) a global semi-empirical approach, in which the main assumption is that the $\phi(\rho z)$ function for a given line in a stratified specimen is almost continuous, like in an homogeneous specimen, even in the presence of strong atomic number variations from one layer to an other. The second assumption is that each one of the four parameters which are needed to describe analytically the $\phi(\rho z)$ function is the same as that of a fictitious homogeneous specimen which would have an average atomic number evaluated by applying a specific weighting law to the layers of the real specimen. The full development of this approach has been done by the author and co-workers for the PAP and the XPP $\phi(\rho z)$ models [7], which are available in the STRATA and STRATAGem programs. The same type of approach has been used later by Bastin [8] for his TFA program and by Merlet [9] for his XPhi program. This kind of global approach enables a fast computation of the k-ratios for any particular problem (less than 1 second). Hence, it permits to perform in a few seconds the tens of iteration loops needed to solve automatically a real problem of composition and thickness determination, even in complex stratified structures. Presently, the semi-empirical $\phi(\rho z)$ approach is unambiguously the most widely used to characterise stratified specimens by X-ray microanalysis. The most questionable point in this approach is the validity of the basic assumption about $\phi(\rho z)$ continuity, in the cases where strong atomic number changes are occurring inside the specimen.

(ii) an other approach initially used by Reuter [16], and later developed by August et al. [17] and Staub [18], is a macroscopic numerical model based on the computation of the energetic and angular distribution of the penetrating and backscattered electrons in the successive elementary layers that can be piled-up to describe the specimen. In principle, this approach should lead to more realistic $\phi(\rho z)$ functions than the previous one, since it takes fully into account the possible atomic number changes at the interfaces and doesn't make any hypothesis of continuity. Although this approach has proved to give good results [18], it doesn't seem to be widely used by the microanalysis community.

(iii) the last approach, which in fact has been the first to give satisfactory results, is the simulation by Monte-Carlo calculations of the electron interactions with the target atoms. As opposed to the case of homogeneous specimens, for which simulations based on multiple scattering schemes are able to give satisfactory

results [19], the case of stratified specimens requires the electron trajectory to be divided in the shortest possible steps, which means that the simulation should be based on a single scattering procedure. Moreover, to hopefully obtain more reliable results, it is recommended to use the complex Mott cross-sections for the elastic scattering rather than a simple screened Rutherford model, and to simulate all kinds of possible interactions as individual statistical events, without using any global law such as the mean energy loss per unit path. Several authors have developed complex simulations of this type [20, 21, 22]. The Monte-Carlo results presented later is this paper have been obtained with a program of this kind [23, 24], taking into account 4 types of individual interactions: the elastic scattering using Mott's cross-sections based on the Salvat's potential [25], the ionisation of atomic levels using Gryzinski's expressions [26], the plasmon excitation according to Ashley and Ritchie [27], and the production of electron-hole pairs according to the model of Ritchie et al. [28]. Both primary incident electrons and fast secondary electrons generated are considered in the simulation. It should be mentioned that in the context of the present paper, this program has the interest of being a purely theoretical computation, without any attempt to adjust some of the parameters on the basis of a particular set of microanalysis results. The drawback of the Monte-Carlo calculations is that they still remain time-consuming, in spite of the increasing speed of personal computers: to construct a statistically well-defined $\phi(\rho z)$ function by taking into account all individual interactions (without any averaging), several hundreds of thousand trajectories have to be simulated, which may lead to a computing time of at least one hour for a single particular condition (voltage, structure, composition). The number of necessary trajectories can be reduced to $\sim 10^5$ if the $\phi(\rho z)$ function is computed by averaging the ionisation production, on the basis of the spatial and energetic distribution of the incident electrons resulting from the simulation, combined with the ionisation cross-section for the level of interest. The Monte-Carlo results presented here have been obtained by this latter method, which leads to a typical computation time not exceeding 1000 seconds for the highest accelerating voltages.

- Most of the information about the accuracy of a given model for layered specimen analysis can be obtain by considering simple specimens. For example, a single layer (even of a pure element) on a substrate is quite suitable to verify that the model to be checked gives the expected mass thickness, that this result doesn't vary too much when the operating conditions (accelerating voltage and possibly analytical line) are changed, and that the results obtained by measuring the radiations of the layer and of the substrate are coherent.
- The first example is based on measurements from Bastin et al. [29]. It illustrates the case of a film which can be considered as thin compared to the depth of ionisation, i.e. an aluminium film with a thickness less than 100 nm analysed with 20 keV electrons (in such conditions, the maximum depth of ionisation is of the order of 4 μm). Bastin et al. measured the k-ratio of such a film as a function of the atomic number Z_{sub} of the substrate, from $Z_{sub} = 4$ (Be) to $Z_{sub} = 83$ (Bi). They reported a thickness of 21.86 μg/cm^2 resulting from RBS measurements. On the other hand, they found 25.56 μg/cm^2 using EPMA in combination with their own thin-film program. Applying our XPP model to this problem, we obtain the best global agreement with Bastin's experimental data for a thickness of 23.0 μg/cm^2. Using our Monte-Carlo program mentioned previously, we find the best overall agreement for 25.9 μg/cm^2. With these values, Fig. 8 shows that both XPP model and Monte-Carlo computations reflect satisfactorily the measured variation of the Al Kα k-ratio with Z_{sub}. Here, it should be pointed out that both procedures of computation that we are applying are totally independent of the selected experimental data. In other terms, these experimental data have never been taken into account to adjust the models used. This is why this comparison is probably a realistic image of the actual uncertainties when trying to determine the absolute value of a mass thickness, not because of the experimental errors, but mostly because of the limitations of the models available. In the present case of a thin surface film, the smallest average deviation to the RBS

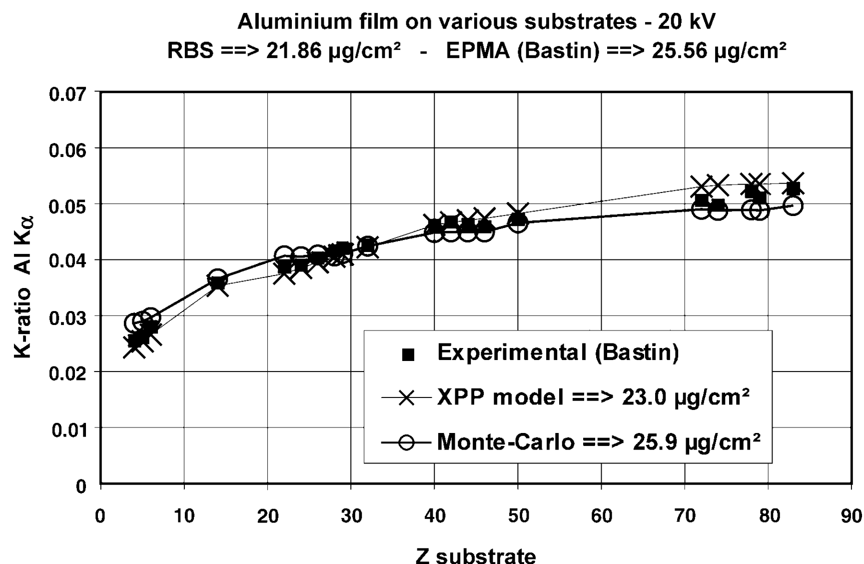

Fig. 8. k-ratio variation of a $\sim 25\,\mu g/cm^2$ aluminium layer as a function of the atomic number of the substrate, from $Z = 4$ to $Z = 83$. Comparison of the results obtained using the XPP model ($23.0\,\mu g/cm^2$) and Monte-Carlo simulation ($25.9\,\mu g/cm^2$) with the measurements of Bastin et al. at 20 kV

determination (~5% r.m.s.) is obtained with the XPP model.

– A second example selected from the measurements of Bastin et al. [30] is a palladium film analysed at 10 kV. Here, the reported thickness resulting from RBS was $44.9\,\mu g/cm^2$, i.e. the film was not thin compared to the depth of ionisation: in fact, this thickness is approximately 1.5 times the depth where the $\phi(\rho z)$ function has a maximum. This kind of situation, where the interface is in the vicinity of the depth of complete scattering, is particularly difficult for the global $\phi(\rho z)$ models when a strong variation of the atomic number is occuring there. Applying their own thin-film program, Bastin et al. found a mass thickness of $48.21\,\mu g/cm^2$. With our XPP model and our Monte-Carlo simulation, we find respectively $45.4\,\mu g/cm^2$ and $43.0\,\mu g/cm^2$. In this case, the variation with Z_{sub} of the Pd Lα k-ratio is perfectly predicted by the Monte-Carlo calculation (Fig. 9), whereas the XPP model is less satisfactory. However, in the average, the XPP model gives a result closer to the RBS one than other determinations. This second example confirms, in the difficult case of a thicker film, the order of magnitude (less than 10%) of the uncertainties of the mass thickness determination.

– In practice, when layers made of a mixture of several elements have to analysed, i.e. when a simultaneous determination of layer thickness and composition has to be done, most of the uncertainty is on the thickness determination, but not on the composition. Since the level of uncertainty is almost the same for all the elements of a layer (except in extreme cases where the energy or the absorption of the characteristic lines involved differ very strongly), the normalisation to 100% of the sum of the concentrations, which has obviously to be done to derive the layer mass thickness, holds most of the uncertainty in the mass thickness determination.

– The next example in Fig. 10 gives an opportunity to show typical variations with the voltage of the k-ratios for layer and substrate elements, in a situation where the atomic number of both constituents do not differ strongly. This is also an opportunity to show that reliable measurements can be made by EDS, at least when the k-ratios are sufficiently high. Here, an aluminium layer with a thickness of the order of 100 nm has been deposited on a silicon oxide substrate. The k-ratios for Al Kα, Si Kα and O Kα lines have been measured at variable electron energy, with a 35° take-off angle. Pure standards are used for Al and Si, and a conductive $Y_3Fe_5O_{12}$ standard is used for the oxygen measurements. Figure 10 shows that the curves corresponding to the thickness of $30\,\mu g/cm^2$ obtained by automatic iterative procedure in the STRATAGem program (using the XPP model) fit remarkably well the experimental k-ratios for all three elements in a wide voltage range. On the other hand, Monte-Carlo calculations (which use the same set of mass absorption coefficients) are in good agreement with the experiment for Al and Si radiations, but the simulation predicts lower

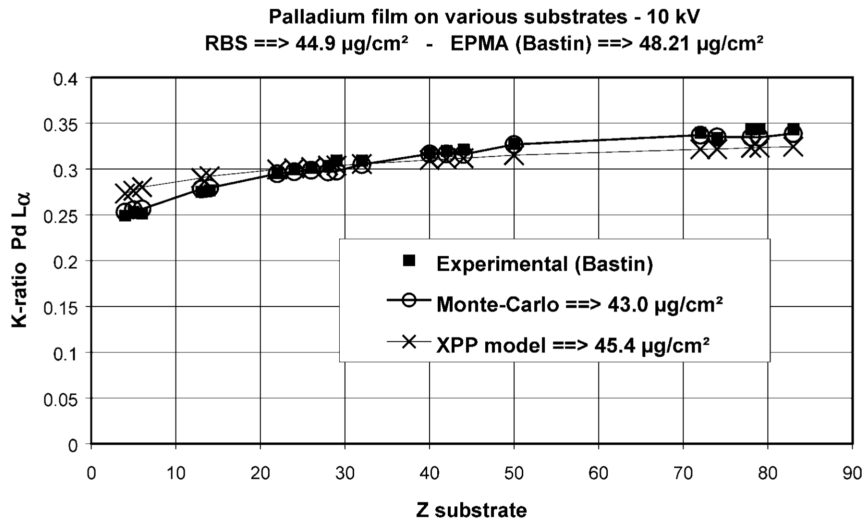

Fig. 9. k-ratio variation of a $\sim 45\,\mu g/cm^2$ palladium layer as a function of the atomic number of the substrate, from $Z=4$ to $Z=83$. Comparison of the result obtained using the XPP model ($43.0\,\mu g/cm^2$) and Monte-Carlo simulation ($45.4\,\mu g/cm^2$) with the measurements of Bastin et al. at 10 kV

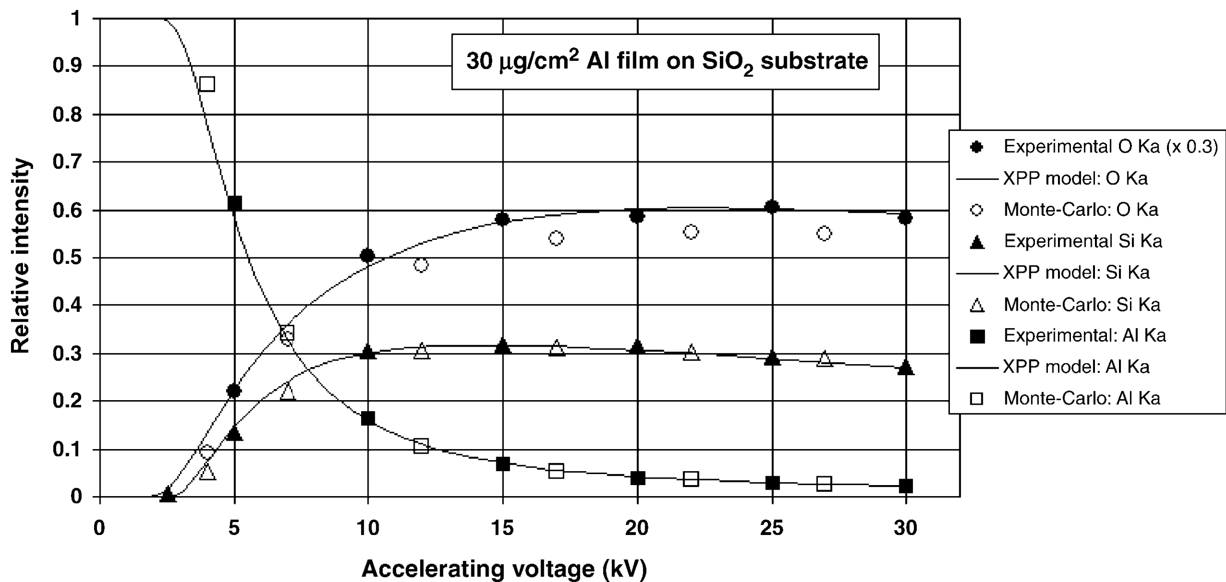

Fig. 10. Aluminium layer ($\sim 30\,\mu g/cm^2$) on silicon oxide substrate. Comparison of the k-ratios measured by EDS at 35° take-off with the XPP curve obtained by automatic iteration in the STRATAGem program, and with Monte-Carlo predictions. (Pure standards for Al and Si, conductive $Y_3Fe_5O_{12}$ for oxygen)

k-ratios for oxygen (the deviation is $\sim 10\%$ relative). Obviously, the case of the oxygen line is the most difficult here, since its higher absorption in Al ($\mu/\rho = 6900\,cm^2/g$) and in Si ($\mu/\rho = 8790\,cm^2/g$) makes it more sensitive to any difference in the shape of the $\phi(\rho z)$ function from one theoretical procedure to another, but also to any distortion of the actual distribution in the insulating substrate, that could result from charge accumulation. In fact, in this particular case of oxygen measurement, the surprisingly good agreement of XPP with the experimental data could simply be a lucky coincidence, where model imperfections could more or less be compensated by uncontrolled effects inside the specimen.

– Now, the most questionable point about the global analytical $\phi(\rho z)$ models is the limit of validity of the assumption made about the continuity of the distribution, in the case of strong changes of mean local atomic number inside the layered specimen. To illustrate this point, we have chosen to consider the case of a film of a heavy element (hafnium) on a low-Z substrate (silicon). In addition, this kind of specimen has the potential of being able to give an

answer to the question about the value of the absorption of Si Kα line by Hf, since the energy of Si Kα (1.740 keV) is close to the Hf M_{IV} absorption edge (1.716 keV). To evaluate the importance of the possible discontinuity in the actual $\phi(\rho z)$ distribution of the radiation, Monte-Carlo simulations have been done for the Hf Mα radiation, between 7 and 40 kV, in the case of a layered specimen with 130 $\mu g/cm^2$ Hf on top of a Si substrate, and in the case of pure Hf for comparison. At 7 kV, 130 $\mu g/cm^2$ represent a major fraction of the ultimate ionisation depth; hence, the layer is appearing as thick, and there is no doubt that the $\phi(\rho z)$ function will be very close to that of pure Hf. On the contrary, at 40 kV, the layer represents a few percent of the ultimate ionisation depth; hence, it looks thin, and there is no doubt that $\phi(\rho z)$ will not be very different from that of Hf Mα in pure Si. The questions about $\phi(\rho z)$ concern the intermediate situations (typically 20 kV in this example), where the layer-substrate interface lies in the vicinity of the maximum of $\phi(\rho z)$. Figs. 11 to 15 give respectively at 7, 10, 20, 30 and 40 kV the comparison of the Hf Mα $\phi(\rho z)$ functions in the pure and in the

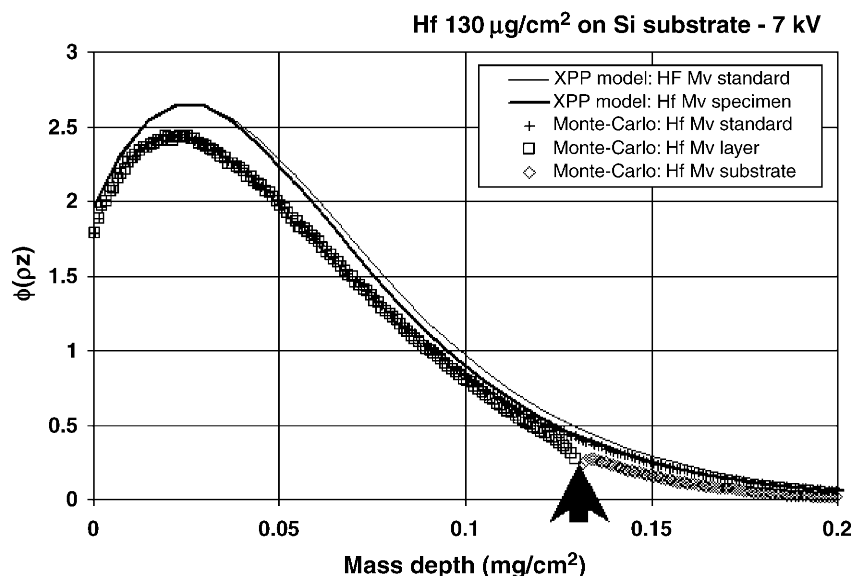

Fig. 11. Hafnium layer (~130 mg/cm^2) on silicon substrate. Comparison of the Hf Mα $\phi(\rho z)$ curves predicted at 7 kV by XPP model and Monte-Carlo simulations, in the layered specimen and in the pure Hf standard

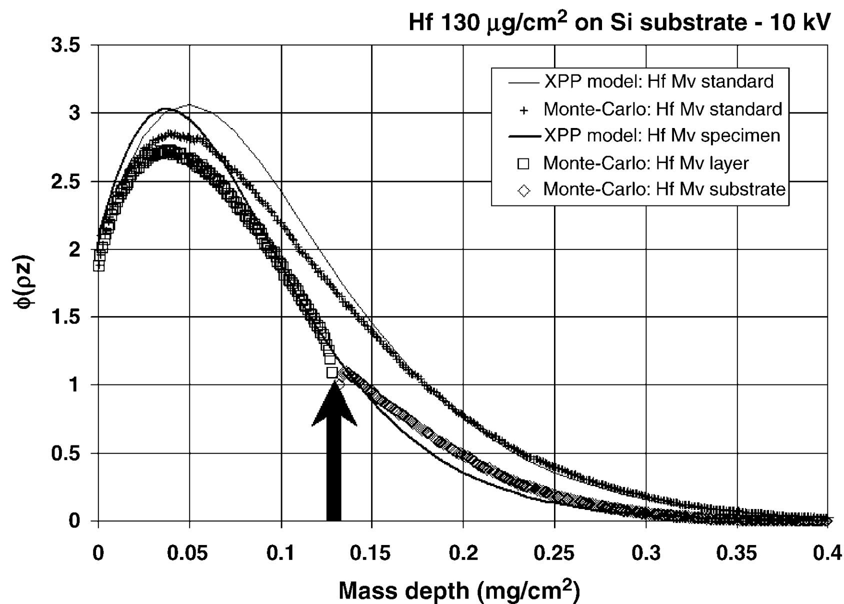

Fig. 12. Hafnium layer (~130 mg/cm^2) on silicon substrate. Comparison of the Hf Mα $\phi(\rho z)$ curves predicted at 10 kV by XPP model and Monte-Carlo simulations, in the layered specimen and in the pure Hf standard

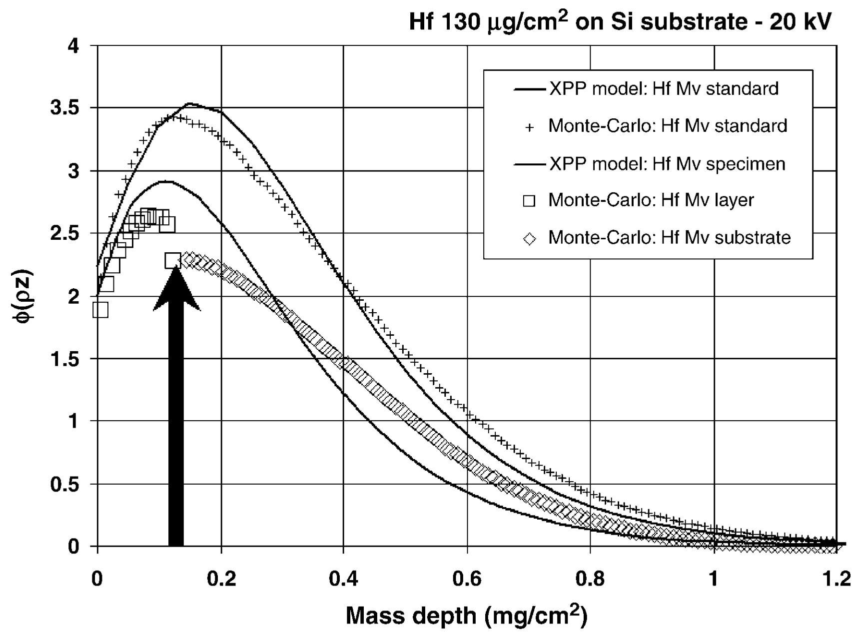

Fig. 13. Hafnium layer ($\sim$130 mg/cm^2) on silicon substrate. Comparison of the Hf Mα $\phi(\rho z)$ curves predicted at 20 kV by XPP model and Monte-Carlo simulations, in the layered specimen and in the pure Hf standard

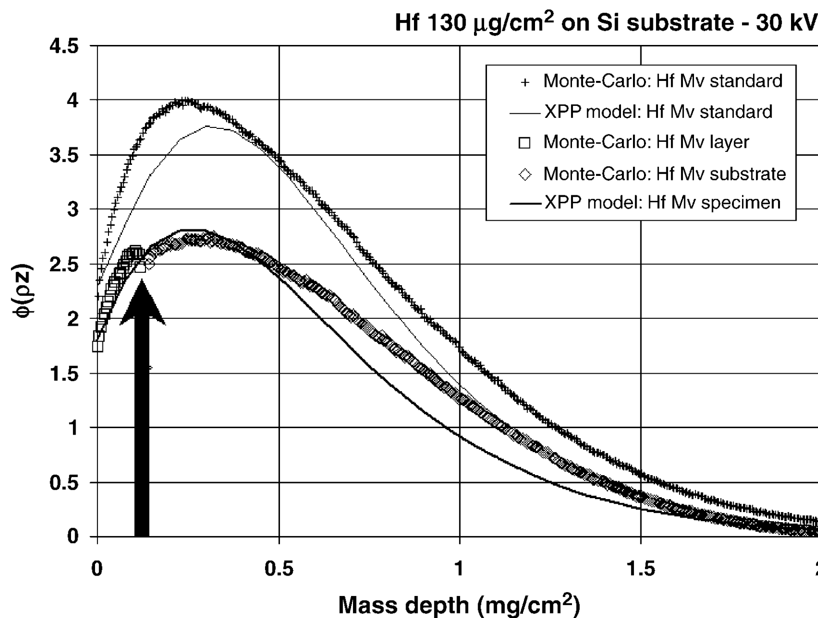

Fig. 14. Hafnium layer ($\sim$130 mg/cm^2) on silicon substrate. Comparison of the Hf Mα $\phi(\rho z)$ curves predicted at 30 kV by XPP model and Monte-Carlo simulations, in the layered specimen and in the pure Hf standard

layered specimen, as predicted by the continuous XPP model and by the Monte-Carlo calculation. In most cases, the assumption of a continuous $\phi(\rho z)$ function appears to be acceptable, except when the interface is in the vicinity of the depth of complete scattering, i.e. at 20 kV for the specimen considered. Apart from this discontinuity and some difference in the scaling of the function (mainly due to a different behaviour, at high overvoltage, of the expressions for the ionisation cross-section used in the XPP model and in the Monte-Carlo simulation), it can be seen that the curves predicted by XPP and Monte-Carlo are globally in good coherence, and that the differences between both methods are almost the same for the pure specimen as for the layered structure. Hence, very comparable ratios could be obtained with both methods when dividing a partial integral for the specimen by the corresponding partial integral for the standard.

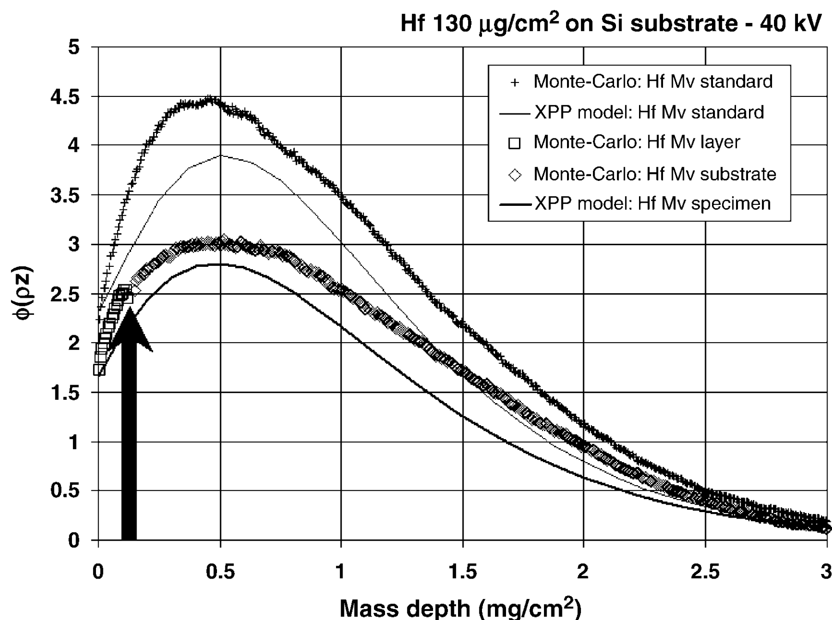

Fig. 15. Hafnium layer ($\sim$130 mg/cm^2) on silicon substrate. Comparison of the Hf Mα $\phi(\rho z)$ curves predicted at 40 kV by XPP model and Monte-Carlo simulations, in the layered specimen and in the pure Hf standard

It is now interesting to see what kind of results are obtained when the $\phi(\rho z)$ model XPP and the Monte-Carlo simulation are applied to this particular specimen. Before entering into the details, one can see in Fig. 16 that both computations agree globally well with the experimental k-ratios for the Si Kα radiation of the substrate. This gives immediately the answer about the absorption: there is no reason to suspect that the value employed for the absorption of Si Kα by Hf ($\mu/\rho = 5061$ cm^2/g, according to Heinrich) could be wrong, unlike what other experiments with hafnium oxide layers could lead to conclude [31]. To confirm this point, we have made a series of similar measurements on a specially elaborated HfO_2/Si specimen, and obtained the same type of agreement between the experiment and the computation, which means that the chemical bonding in the oxide doesn't produce any detectable change in the absorption coefficient of Si Kα by Hf atoms.

The second conclusion is that the strong difference in the atomic numbers of the Hf layer and the Si substrate doesn't seem to produce significant errors, since the XPP curves agree globally rather well with both sets of experimental data, although the fit is not absolutely perfect over the whole range of accelerating voltage investigated. The third point is quite surprising: because of the assumption of $\phi(\rho z)$ continuity made in the XPP model, we would expect a maximum discrepancy around 20 kV, as discussed before. In the vicinity of this medium-range voltage, we

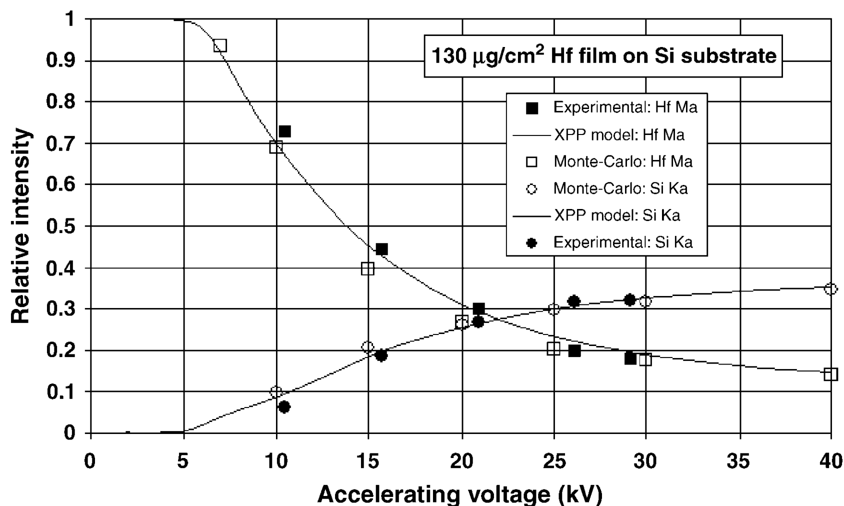

Fig. 16. Hafnium layer ($\sim$130 mg/cm^2) on silicon substrate. Comparison of the values obtained using XPP model and Monte-Carlo simulation with the Hf Mα and Si Kα k-ratios measured at 40° take-off by WDS

also would expect the Monte-Carlo simulation to be much more accurate than any global $\phi(\rho z)$ model. On the contrary, it can be seen that actually, the deviation of Monte-Carlo results from experimental data is maximum in the vicinity of 20 kV: for reasons not well understood, Monte-Carlo results seem to be fairly accurate below 10 kV and above 30 kV, but predict too low k-ratio values (more than 10% relative deviation) for the layer signal at intermediate voltage.

Strategy for the Analysis of Layered Specimens

Giving a general strategy for analysing layered specimens is almost impossible, since there is an infinity of situations depending on the structure of the specimen (number and thickness of layers), the nature and the concentration of the elements in each of them, the fact that some elements can be simultaneously present (or not) in several layers, and the knowledge (or absence of knowledge) of some particular features of the specimen, such as the sequence of piling-up, the presence (or absence) of a given element in a particular layer, the composition of particular layer(s) or substrate, etc.

If the sequence of layer stacking is not *a priori* known, a sufficient number of measurements at variable voltage for all the detectable elements will be necessary to deduce a realistic hypothesis about this sequence, which is indispensable to any further attempt of quantification.

Assuming now that the stacking sequence is known (i.e. the number of layers and the distribution of the elements in these layers and the substrate are known), the simplest situation is realised when every element is present in only one of the components of the layered structure. In such a case, k-ratio measurements made for all elements at a sufficiently high single voltage are in principle sufficient to obtain simultaneously the mass thickness of all layers and the compositions of all the components of the structure, including the substrate. In a situation of this type, there is no danger to apply a simple iteration scheme, which uses the sum of the k-ratios of the elements present in a layer to derive its mass thickness and the normalised k-ratios to obtain the composition [5].

All other cases where some elements are simultaneously present have to be tackled by a trial and error procedure, aiming to minimise the deviation between the k-ratios computed for a particular hypothesis about the specimen and a set of experimental k-ratios acquired in a wide and well-chosen range of accelerating voltage. In such situations, good results can be obtained with a complex iterative scheme which looks for the minimum deviation, but in some unfavourable cases, there is some danger to find a local minimum instead of the true minimum of the deviation. Hence, it is not advisable to overlook verifying "by hand" the sensitivity of the computed k-ratios to particular thickness or composition changes. Moreover, for peculiar specimen structures, it can be necessary to perform measurements for a given element using characteristic lines of two different series. Figure 17 illustrates such a situation for a Cu/Ni/Cu multi-layer on Si substrate, in the case where the Cu film at the surface is very thin (less than 2 nm), while the buried Cu film is quite thick (about 900 nm), both Cu layers being separated by a $\sim$ 50 nm Ni layer. If the Cu Kα signal was used alone, the contribution

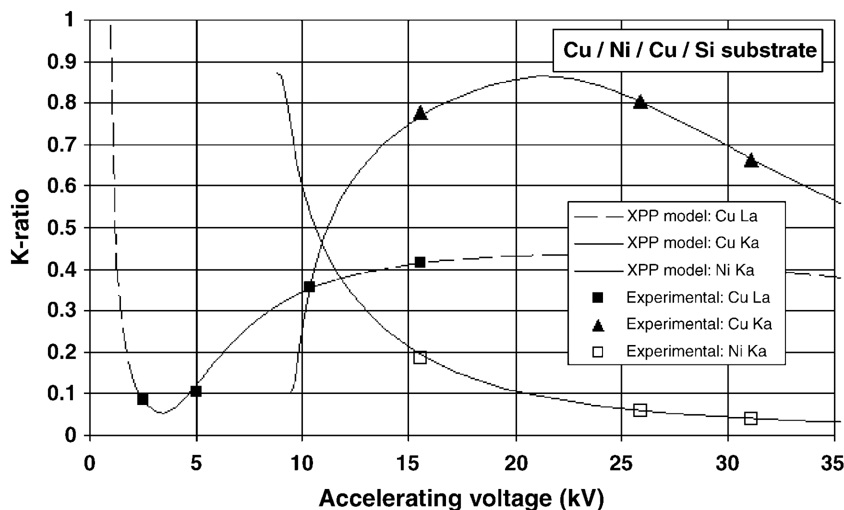

Fig. 17. Use of two different characteristic lines (Cu Kα and Cu Lα) for the discrimination between a thin surface layer and a thick buried layer of the same material. Specimen structure: Cu 1.5 $\mu g/cm^2$/Ni 46 $\mu g/cm^2$/Cu 803 $\mu g/cm^2$/Si substrate

of the thin surface film would be completely masked by that of the thick buried layer. On the contrary, by measuring also the Cu Lα k-ratio at low voltage, the existence of the Cu surface film can be revealed. Since the STRATAGem program permits to process simultaneously several lines for a single element, an automatic processing of the data can be done. It gives a surface Cu segregation in very good agreement with that found on a reference (Cu/Ni/Si substrate) elaborated simultaneously. The XPP curve in Fig. 17 corresponds to this best adjustment, obtained for the following description: Cu 1.5 $\mu g/cm^2$/Ni 46 $\mu g/cm^2$/ Cu 803 $\mu g/cm^2$/Si substrate.

Conclusion

A sufficient experience of X-ray microanalysis applied to surface films and layered specimens has now been accumulated to consider the method becoming mature. It can be applied to the characterisation of very thin surface segregations (in a low-voltage operation mode), or to the simultaneous determination of thickness (in the sub-micron range) and composition of surface layers, buried layers or substrates, provided that the operating conditions are correctly adapted to any particular problem. In principle, its accuracy is certainly comparable to that of the RBS method, but as in any method, the practical level of performance is essentially dependent on the complexity of each particular specimen to be characterised. Lacking information about the specimen structure, it may be tedious to perform the all the necessary measurements which can lead to a realistic hypothesis about the structure. On the contrary, in the cases where sufficient knowledge is available about the specimen configuration, the method may be used as a routine control tool. In all cases however, and specially when low-energy radiation is used for the measurement of thin segregations, sufficient skill is necessary to avoid all the possible pitfalls. Although efficient automatic procedures for processing the data are available in some commercial software packages and may be applied to a limited set of experimental data, it is recommended to acquire a set of k-ratios in a sufficiently wide range of accelerating voltage, and not to disregard the "manual" processing mode because it permits to anticipate some problems before doing the experiment, and also permits to have a critical appraisal of one's own conclusions after the experiment.

Some examples of measurements made in the situation where the assumptions of global $\phi(\rho z)$ models are in principle the most questionable (i.e. strong atomic number difference between adjacent layers in the vicinity of the depth of complete scattering) seem to demonstrate that the level of uncertainty, when such models are applied in the most difficult conditions, is not critical and that more sophisticated and time-consuming approaches such as Monte-Carlo simulations don't give systematically more reliable results.

Acknowledgements. The author acknowledges his collaborators Denis Boivin et Yves Pioche for their contribution to some of the measurements, and to Stéphane Landais for preparing the hafnium layers. Special thanks are due to Dr Jean Henoc for his major action in the development of the Monte-Carlo program and for lively discussions.

References

[1] J. Philibert, D. Penot, *X-Ray Optics and Microanalysis*, Proc. ICXOM 4. In: Castaing, Deschamps, Philibert (Eds.) Publ. Hermann, Paris, 1966, p. 365.
[2] J. L. Pouchou, F. Pichoir, *La Recherche Aérospatiale* **1984**, *5*, 47.
[3] J. L. Pouchou, F. Pichoir, *Scanning* **1990**, *12*, 212.
[4] J. L. Pouchou, *Anal. Chim. Acta* **1993**, *283*, 81.
[5] J. L. Pouchou, F. Pichoir, *Scanning Microscopy* [*Suppl.*] **1993**, *7*, 167.
[6] P. Willich, *J. Microsc. Spectrosc. Electron*. **1985**, *10*, 269.
[7] J. L. Pouchou, F. Pichoir, *Electron Probe Quantitation*. In: Heinrich & Newbury (Eds.) Plenum Press, New York, 1991, p. 31.
[8] G. F. Bastin et al., *Microbeam Analysis*. In: Bailey & Rieder (Eds.) San Francisco Press, 1993, p. 2.
[9] C. Merlet, *Microbeam Analysis*. In: Etz (Ed.) VCH Publ., 1995, p. 203.
[10] S. J. B. Reed, *Brit. J. Appl. Phys*. **1965**, *16*, 913.
[11] J. L. Pouchou, *Mikrochim. Acta* **1994**, *114/115*, 33.
[12] J. L. Pouchou, *Mikrochim. Acta* [*Suppl.*] **1996**, *13*, 39.
[13] J. L. Pouchou, F. Pichoir, *Microbeam Analysis*. In: Newbury (Ed.) San Francisco Press, 1988, p. 319.
[14] K. F. J. Heinrich, *Proc. ICXOM 11*. In: Brown & Packwood (Eds.) Publ. Univ. Western Ontario, 1986, p. 67.
[15] R. Castaing, *Thesis*, Univ. Paris, 1951.
[16] W. Reuter, *Proc. ICXOM 6*. In: Shinoda, Kohra, Ichinokawa (Eds.) Univ. Tokyo Press, 1972, p. 121.
[17] H. J. August, J. Wernisch, *X-Ray Spectrom*. **1991**, *20*, 131.
[18] P. F. Staub, *Microanalyse X: méthodes de Monte-Carlo et modèles de correction*. In: Fialin, Pouchou, Bresse (Eds.) Publ. ANRT/G8 Paris, 1997, p. F1.
[19] H. Bishop, *Ph. D. Thesis*, Univ. Cambridge, 1965.
[20] R. Shimizu, K. Murata, G. Shinoda, *X-Ray Optics and Microanalysis*, Proc. ICXOM 4. In: Castaing, Deschamps, Philibert (Eds.) Publ. Hermann Paris, 1966, p. 127.
[21] L. Reimer, E. R. Krefting, *NBS Special Publ*. **1976**, *460*, 45.
[22] N. Amman, P. Karduck, *Microbeam Analysis*. In: Michael, Ingram (Eds.) San Francisco Press, 1990, p. 150.
[23] J. Henoc, F. Maurice, F. Pichoir, J. L. Pouchou, *Microbeam Analysis*. In: Friel (Ed.) VCH Publ., 1994, p. 211.

[24] J. Henoc, F. Pichoir, *Microanalyse X: méthodes de Monte-Carlo et modèles de correction*. In: Fialin, Pouchou, Bresse (Eds.) Publ. ANRT/G8 Paris, 1997, p. A1.
[25] F. Salvat, R. Mayol, *Computer Physics Communications* **1993**, *74*, 358.
[26] M. Gryzinski, *Phys. Rev.* **1965**, *138*, A305.
[27] J. C. Ashley, R. H. Ritchie, *Phys. Stat. Sol*. **1970**, *40*, 623.
[28] R. H. Ritchie, C. J. Tung, V. E. Anderson, J. C. Ashley, *Radiat. Res.* **1975**, *64*, 181.
[29] G. F. Bastin, H. J. M. Heijligers, *X-Ray Spectrom.* **2000**, *29*, 212.
[30] G. F. Bastin, H. J. M. Heijligers, *X-Ray Spectrom.* **2000**, *29*, 373.
[31] V. Sammelselg, *J. Anal. At. Spectrom*. **1999**, *14*, 523.